Journal of the European Ceramic Society **14** (1994) 327–335

A New Approach for Slow Crack Growth Measurement

C. Olagnon, J. Chevalier, F. Sudreau* & G. Fantozzi

INSA GEMPPM, URA 341, 69621 Villeurbanne Cedex, France

(Received 17 November 1993; revised version received 11 April 1994; accepted 5 May 1994)

Abstract

A new approach for the analysis of sub-critical crack growth measured by static and dynamic fatigues is proposed. This approach is based on the knowledge of the initial defect size distribution, which is mathematically related to time to failure probability in the case of static fatigue or to the fracture stress probability in the case of dynamic fatigue. This method, which allows the determination of the sub-critical crack growth parameters with a good accuracy with a minimum number of specimens and under a single applied load, has been applied to mullite and zirconia. In the case of the dynamic fatigue test, the sub-critical crack growth parameters can be obtained with a single loading rate or with two close rates for more precision. Under these conditions, the parameters corresponding to the Wrst stage of the standard propagation law can be inferred, making the results relevant for lifetime prediction.

Eine neue Methode zur Analyse des unterkritischen Rißwachstums, ermittelt mit Hilfe statischer und dynamischer Ermüdung, wird vorgeschlagen. Die Methode basiert auf der Beziehung zwischen anfänglicher Defektgrößenverteilung und, im Falle statischer Ermüdung, der Lebensdauerwahrscheinlichkeit oder, bei dynamischer Ermüdung, der Bruchspannung. Dieses Verfahren erlaubt die zuverlässige Bestimmung der unterkritischen Rißwachstumsparameter mit einer geringen Anzahl von Proben bei einem einzigen Lastwert und wurde für Mullit und Zirkoniumoxid angewendet. Im Fall der dynamischen Ermüdung können die unterkritischen Rißwachstumsparameter unter Verwendung einer einzigen Lastrate oder zur Erhöhung der Genauigkeit bei zwei Lastraten bestimmt werden. Unter diesen Bedingungen läßt sich schließen, daß die Parameter, die dem ersten Stadium des Standardwachstumsgesetz entsprechen, zur Bestimmung der Lebensdauer verwendet werden können.

Une nouvelle approche pour l'analyse statistique de la croissance sous critique mesurée par fatigues statique ou dynamique est proposée. Cette approche est basée sur la connaissance de la distribution de tailles initiales de Wssures, qui est mathématiquement reliée à la probabilité de temps à rupture dans le cas de la fatigue statique et à la probabilité de contraintes à rupture dans le cas de la fatigue dynamique. Cette méthode qui permet de déterminer les paramètres de croissance sous critique avec une bonne précision et un minimum d'échantillons a été appliquée à une zircone et une mullite. Dans le cas de la fatigue dynamique, les paramètres de croissance sous critique peuvent être obtenus avec une seule vitesse de chargement ou bien avec deux vitesses proches pour une plus grande précision. Dans ces conditions, les paramètres correspondant au premier stade de la propagation sous critique peuvent être obtenus, ce qui permet de prévoir des durées de vies correctes.

1 Introduction

Numerous methods exist for the measurement and the analysis of the subcritical crack growth in ceramics. These different methods can be practically divided into two groups: (i) direct measurement methods where the crack velocity is recorded as a function of the stress intensity factor and (ii) indirect measurement methods where the shape of the curve needs to be presupposed.

The former methods which include techniques such as double torsion,[1–4] double cantilever[4–7] and bending bars,[5] present the advantage of allowing the determination of the precise shape of the V–K curve and especially the three stages often observed in air. These techniques, however, are

* Present address: CEA, DER/SCC/LECC, 13108 St Paul Lez Durance, France.

Journal of the European Ceramic Society 0955-2219/94/$7.00

relatively complex to carry out and can not be conducted down to extremely low crack velocities with sufficient precision. Moreover the artificial cracks, generally longer than 1 mm, that are introduced, may not be relevant to predict the fatigue behaviour of real flaws.

The latter methods, which include static fatigue,[8,9] dynamic fatigue[5] and even cyclic methods,[10–12] present the advantage of being easy to conduct on specimens of very simple shape. Moreover, static fatigue allows measurements down to extremely low velocities. These methods are generally based on a similar principle. A shape of the V–K curve is presupposed (generally $V = AK_I^n$) and the different parameters of this law are obtained from the fitting of experimental results to the integration of the presupposed law over the stressing condition. In the case of static fatigue standard analysis a series of specimen sets is tested under different constant applied loads and the results in terms of time to failure are plotted on a $\log(t_f)$ versus $\log(\sigma)$ diagram. Under the former hypothesis, the plot should define a straight line of slope $-n$. In the case of dynamic fatigue, a series of specimen sets are tested under different constant loading velocities and the results in terms of stress to rupture are plotted on a $\log(\sigma_r)$ versus log (loading rate) plot that should define a straight line of slope $1/(n+1)$.

Such methods can not separate the different propagation stages and the A and n values represent average values of the three stages investigated. The major problem is that the importance of the respective stages depends either on the time to failure investigated (static fatigue) or on the loading rate (in the case of the dynamic fatigue test).

The case of static fatigue is less critical since it characterizes only the first stage when used with long durations, which is generally of interest for lifetime prediction of real components. However, owing to the dispersion of results, a lot of specimens are generally required for a fine analysis of the static fatigue results, and accordingly the studies are of long duration.

Observing that the standard procedure consists of fitting the median values of given applied stresses, Jakus *et al.*[13] have proposed different refinements of the statistical treatment. They include all the different results in the analysis and therefore improve the precision. Fett and coworkers[14–16] have proposed a modified analysis which presents the main advantage of not requiring any prerequisite on the shape of the sub-critical crack law. This method is based on the scattering of either the initial crack lengths or applied stresses.

The dynamic fatigue test is easy to conduct and of short duration but still requires a significant number of specimens. Moreover, as already mentioned, it can be of low scientific usefulness since it mostly leads to an average value of the different stages. Even if a single stage really operates, the presence of a threshold value or a too high loading rate have been shown to lead to erroneous results.[17,18] Kadouch[18] has shown that in such a case, only a limited range of loading rates could be conducted to obtain relevant results.

The purpose of this paper is to present an original statistical method that was initially applied for thermal fatigue determination.[19] The idea is to introduce artificial defects of known sizes and to use the initial length scattering to obtain the propagation law with a single applied stress in the case of static fatigue and a limited number of specimens. For this target, an analytical function of the failure probability that depends on the test is established and adjusted to the experimental results in order to determine the slow crack growth parameters. The method is also applied to dynamic fatigue. Although it might be theoretically possible to obtain the parameters with a single applied loading rate, a more precise determination will require two loading rates. The first stage parameters will therefore be obtained.

2 Theoretical Background

2.1 Static fatigue application

The prerequisite of the analysis is that the initial flaw distribution is definitely known. For this purpose, artificial defects that can be precisely known are introduced in the specimens. A convenient way is by Vickers indentation, where the initial size can be controlled by the applied load. Under specific loads the initial crack can therefore be of half-penny shape. The Vickers indentation leads to two perpendicular cracks but it may reasonably be assumed that the crack parallel to the load does not induce any perturbation. Such cracks can be shown to fairly fit a Gaussian distribution, which gives the following probability density as a function of flaw size a_i:

$$f_a(a_i) = \frac{1}{S_d(2\pi)^{1/2}} \exp\left(-\frac{1}{2}\left(\frac{a_i - \langle a\rangle}{S_d}\right)^2\right) \quad (1)$$

where $\langle a\rangle$ and S_d respectively the average and standard deviation values.

Considering the static fatigue test where the specimens are submitted to a constant stress σ, the

probability densities of crack size a_i and lifetime t_f are defined as:

$$f_a(a_i) = \frac{P(a_i < a_{io} < a_i + da_i)}{da_i} \quad (2)$$

$$f(t_f) = \frac{P(t_f + dt_f < t_{f0} < t_f)}{-dt_f} \quad (3)$$

where $P(a_i < a_{io} < a_i + da_i)$ and $P(t_f + dt_f < t_{fo} < t_f)$ represent the probabilities that the initial crack size a_{io} and the lifetime t_{fo} are in the range a_i to $a_i + da_i$ and $t_f + dt_f$ to t_f respectively. It is important to note that the smaller the crack size the longer the lifetime. Since the probabilities are equal, eqns (2) and (3) lead to:

$$f(t_f) = -f_a(a_i)\frac{da_i}{dt_f} \quad (4)$$

which relates the probability density of initial crack size to the probability density of time to failure.

The second part of the analysis will therefore consist of expressing the initial size as a function of the parameters of the test and of the time to failure and to insert it into eqn (4).

The crack propagation velocity is related to the stress intensity factor by:

$$\frac{da}{dt} = AK_I^n \quad (5)$$

The stress intensity factor is related to the crack size and the applied stress by:

$$K_I = Y\sigma a^{1/2} \quad (6)$$

Inserting eqn (6) in eqn (5) leads to the standard crack propagation equation:

$$\frac{da}{dt} = A\,Y^n\sigma^n a^{n/2} \quad (7)$$

Integrating the crack size from a_i to a_f during the time 0 to t_f in relation (7) and considering[20] that the final crack size to the power $(2 - n)/2$ is negligible compared to the initial crack size to the same power, yields the crack size as:

$$a_i^{2-n/2} = \frac{n-2}{2} A\,Y^n\sigma^n t_f \quad (8)$$

Derivation of a_i in eqn (8) with respect to t_f and inserting in eqn (4) yields:

$$f(t_f) = f_a(a_i)\left(\left(\frac{n-2}{2}\right)^n A^2 (Y\sigma)^{2n} t_f^n\right)^{1/(2-n)} \quad (9)$$

Inserting the probability density of initial crack size eqn (1) in eqn (9) gives the probability density of lifetime:

$$f(t) = \frac{\left(\left(\frac{n-2}{2}\right)^n A^2 \cdot (Y\sigma)^{2n} t_f^n\right)^{1/(2-n)}}{Sd\sqrt{2\pi}} \times \exp\left(-\frac{\left(\left(\frac{n-2}{2}\cdot A(Y\sigma)^n t_f\right)^{2/(2-n)} - \langle a\rangle\right)^2}{2S_d^2}\right) \quad (10)$$

Accordingly, the cumulated failure probability of lifetime is obtained by integrating relation (10):

$$F(t_{fc}) = \int_0^{t_f} f(t_f)\,dt_f \quad (11)$$

The failure probability is therefore explicitly known and is a function of the parameters Y, $\langle a\rangle$, S_d, σ, A and n. The initial crack size distribution can be measured, and the applied stress is precisely known. The initial value of the Y parameter can not be precisely known, but with a higher precision than natural defects. The value is slightly varying with crack propagation during the test. However, if not too extended crack propagation is experimentally obtained, the variation does not exceed a few percent, and can be considered as constant as a first approximation. The only adjustable values in the theoretical function (11) are therefore the A and n parameters of the subcritical crack growth law eqn (5).

Experimental time to failure results can be classified and a failure probability $P_i(t_{fi})$ can be attributed. The fitting of these experimental results by the theoretical failure probability, by a least-squares procedure, will therefore lead to the values of the A and n parameters. Note that a single applied stress value is required.

2.2 Application to dynamic fatigue

The former analysis can be applied to dynamic fatigue test after few modifications. Again artificial cracks are introduced in the specimens and they obey the density of probability eqn (1). The results are now represented in terms of the failure stress σ_r. The density of probability of fracture stress is given by:

$$f(\sigma_r) = \frac{P(\sigma_r + d\sigma_r < \sigma_{ro} < \sigma_r)}{-d\sigma_r} \quad (12)$$

where $P(\sigma_r + d\sigma_r < \sigma_{ro} < \sigma_r)$ represents the probabilities that failure stress σ_{ro} is in the range $\sigma_r + d\sigma_r$ to σ_r. By the same analysis a relation similar to eqn (4) is obtained:

$$f(\sigma_r) = -f_a(a_i)\frac{da_i}{d\sigma_r} \quad (13)$$

The slow crack growth eqn (7) is still valid but the

stress must be replaced by:

$$\sigma(t) = \omega t \tag{14}$$

where ω is the loading rate during the test and t the time. Inserting eqn (14) in eqn (7) and integrating the crack size from a_i to a_f when the stress increases from 0 to the failure stress σ_r under the same simplifying hypothesis $a_i^{(2-n)/2} \gg a_f^{(2-n)/2}$ leads to:

$$a_i^{(2-n)/2} = \frac{n-2}{2n+2} A Y^n \sigma_r^{n+1} \omega^{-1} \tag{15}$$

It should be noted that neglecting the final crack length is here less rigorous than for static fatigue, since the crack propagates over shorter time. Deriving eqn (15) with respect to σ_r and inserting in eqn (13) yields:

$$f(\sigma_r) = f_a(a_i)\left(\left(\frac{n-2}{2n+2}\right)^n \frac{A^2 \cdot Y^{2n}}{\omega^2} \sigma_r^{3n}\right)^{1/(2-n)} \tag{16}$$

Inserting eqn (15) in eqn (1) and in eqn (16) leads to:

$$f(\sigma_A) = \frac{\left(\left(\frac{n-2}{2n+2}\right)^n \frac{A^2 \cdot Y^{2n}}{\omega^2} \sigma_r^{3n}\right)^{1/(2-n)}}{S d\sqrt{2\pi}} \times \exp\left(-\frac{\left(\left(\frac{n-2}{2n+2} A Y^n \frac{\sigma_r^{n+1}}{\omega}\right)^{2/(2-n)} - \langle a \rangle\right)^2}{2S_d^2}\right) \tag{17}$$

Similarly to relation (11) the failure probability can be obtained by integrating relation (17)

$$F(\sigma_{rc}) = \int_0^{\sigma_{rc}} f(\sigma_r)\, d\sigma_r \tag{18}$$

A similar procedure as that presented for static fatigue can therefore be applied to obtain the parameters of the slow crack growth law, A and n. It should be noted that a single loading rate should be theoretically sufficient. In addition to the reduced number of specimens and the increased precision, the method in this last case brings the advantage of theoretically allowing the determination of the slow crack growth law with a sole slow loading rate. This could lead to the determination of the first stage parameters, which is generally not the case by the standard analysis.

3 Applications

3.1 Static fatigue

The method was first applied to static fatigue analysis. For this purpose, two different materials have been selected: a Y-TZP zirconia (Ceramiques Techniques Desmarquest, France) and a mullite material (Ceraten, Spain). It should be noted that these two materials should not experience any R-curve behaviour that could perturb the analysis. Indeed, it has been shown[21] that, in the case of R-curve material, the difference between the crack propagation of micro- or macro-defects is significant. Starting from artificial defects would therefore lead to data irrelevant for the lifetime prediction of real components.

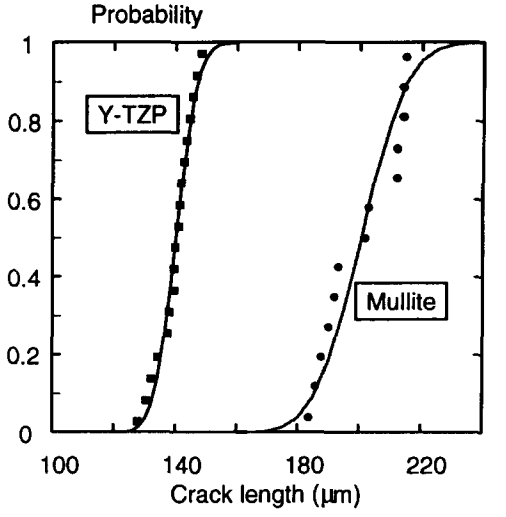

Fig. 1. Initial crack length distributions fitted by Gaussian laws.

The mullite selected here is a brittle material that does not exhibit any R-curve behaviour. Y-TZP is acknowledged to exhibit a strong reinforcement by transformation toughening and to exhibit R-curve behaviour. However the crack resistance is also difficult to measure because it extends over only few microns and this material is therefore often considered as a flat R-curve material.[22]

Both materials were cut into bars of section 6 × 4 mm^2 and polished down to a 3 μm grit. The artificial defects were made by Vickers indentation under loads of 100 N for the zirconia and 60 N for the mullite material. After checking that half-penny shape cracks were made, the surface length was measured by optical microscopy. Figure 1 shows that both series of crack lengths can be fitted fairly well to a Gaussian law. Such a distribution law presents the advantage of being described by only two parameters, the average and the standard deviation that are quoted in Table 1. The mullite specimens were heated to 1000°C for 1 h in order to anneal the residual stress. This could not be done in the case of the zirconia material

Table 1. Average and standard deviation values of the initial crack length distribution initiated by Vickers indentation on the mullite and the zirconia material

Material	*Vickers load (N)*	*Average size (μm)*	*Standard deviation (μm)*
Y-TZP	100	140	6
Mullite	60	200	12

since the heat treatment was shown to induce some crack healing.[22]

3.1.1 Application to Y-TZP

The statistical analysis described in the theoretical section has been applied. For this purpose, 20 specimens were tested at 132·5 MPa and the different times to failure t_i were recorded. The experimental failure probability has been attributed, after classification of the different times to failure, by the following expression:

$$P_i(t_i) = \frac{i - 0{\cdot}5}{20} \tag{19}$$

The experimental time to failure probability was therefore expressed as:

$$P_i = \text{function } (t_i) \tag{20}$$

The results are displayed in Fig. 2. The theoretical probability of time to failure expressed by the relation (11) depends on the two parameters A and n that can be adjusted in order that the theoretical probability fits the experimental one. This is achieved by a least squares procedure, i.e. by minimizing the following relation:

$$S = \sum_{i=1}^{N} [F(t_{fi}, n, A) - P_i(t_{fi})]^2 \tag{21}$$

where N represents the number of tested specimens. The minimum value was found for parameters values of $A = 0{\cdot}99 \times 10^{-18}$ and $n = 26$.

The first question that arises is the problem of the uniqueness of the solution. This has been investigated by calculating the parameter S for a wide range of (n, A) values. It appears that for a given n value, the graph of S versus A exhibits

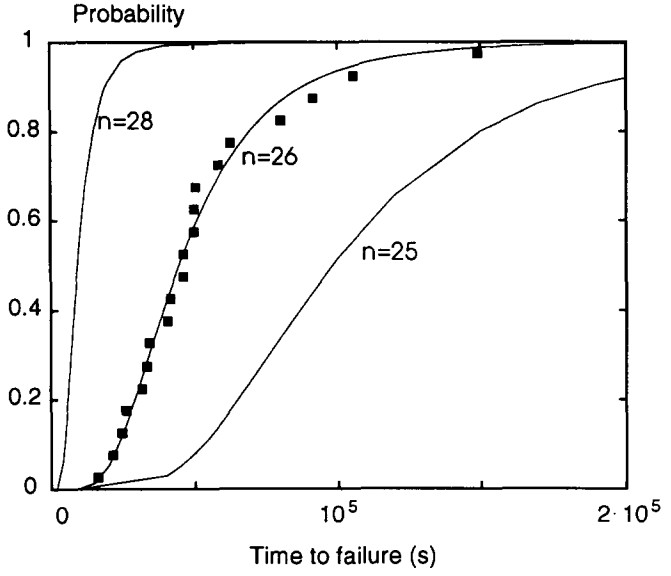

Fig. 2. Fitting of the experimental time to failure probability of the Y-TZP material by the theoretical probability of failure under an applied stress of 132·5 MPa. By adjusting A and n the best fitting can be obtained.

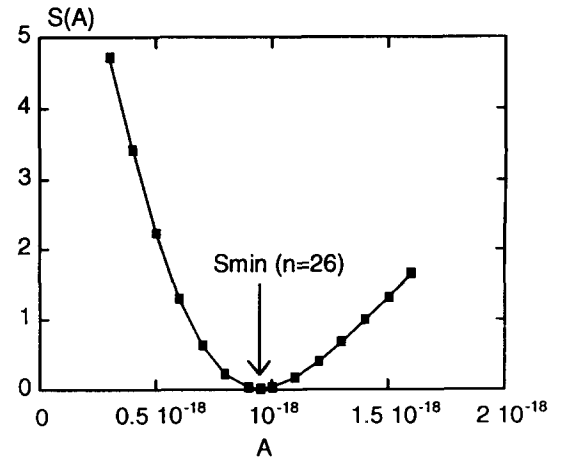

Fig. 3. S as a function of the parameter n for different couples (A, n) in order to find the minimum value.

a marked minimum (Fig. 3). Conversely, a clear minimum of the $S(n)$ graph is obtained for a fixed A value. The representation of these minima in the $\log(A)$ versus n graph which is displayed in Fig. 4 surprisingly defines a straight line. Along this line, the variation of S also shows a minimum (Fig. 5) but that is less marked. In fact, it does correspond to the uncertainties over the A and n values. It therefore implies that a range of (A, n) couples fits the experimental results fairly well.

In order to demonstrate the validity of this method, the standard procedure analysis requiring several applied stresses was also applied in the case of the zirconia material. For this purpose, the indented specimens were submitted to three different stresses σ_a, and the times to failure t_f were recorded. The results are displayed in Fig. 6. It is to be noted that the second series of specimens (applied stress of 132·5 MPa) contains a larger number of specimens, since it has been used to illustrate the new method. The different results were plotted on a standard log t_f–log σ_a diagram whose slope can give the stress exponent of the

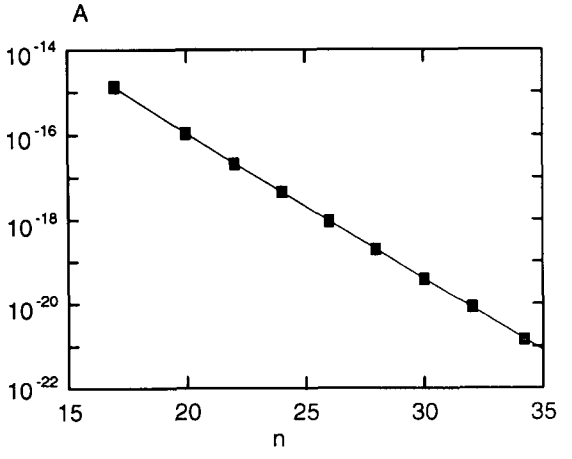

Fig. 4. Fitting of the experimental time from the theoretical curve. Representation of the optimum value of A for a given value of n. Along this line the variation of S is relatively smooth.

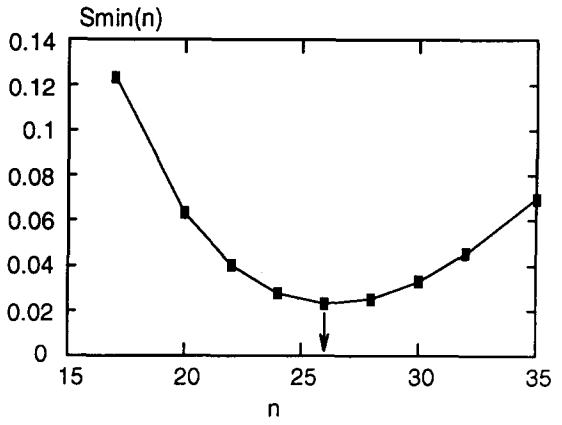

Fig. 5. Representation of the minimum value of $S(A, n)$ as a function of the parameter n. This corresponds to the values of S along the straight line displayed in Fig. 4.

propagation law n. A least squares linear regression leads to $A = 4{\cdot}32 \times 10^{-17}$ and $n = 20{\cdot}6$. Since the initial defect sizes were known, the second parameter A of the propagation law can be obtained.

The V–K curve can subsequently be represented and compared with results obtained from the standard analysis. This has been achieved in Fig. 7 where the results measured by double torsion on the same material has also been plotted. Both the static fatigue results obtained from the standard analysis and the new approach proposed here appear to lead to relevant data, at least when compared with double torsion. It is to be noted, however, that the new method seems to lead to more discrepancy. However, since the comparison with double torsion can only be made by extrapolating the results to lower values, it is difficult to affirm which data are better. Indeed, it should be recalled that while the standard analysis is conducted with different applied stresses, the new method is applied with a single applied stress. The range in crack velocities investigated might therefore be different.

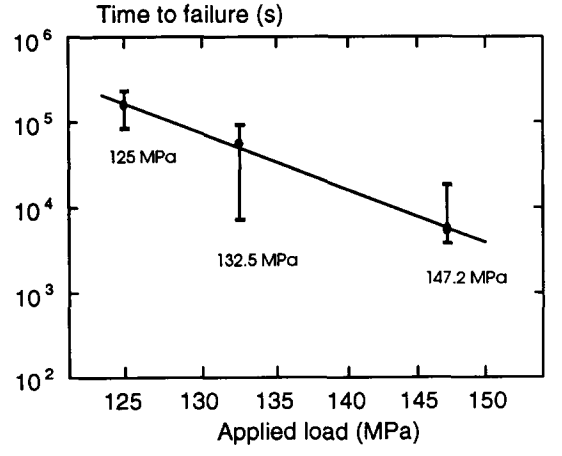

Fig. 6. Analysis of the static fatigue by the standard method. The point represents the average value, and the bars give the maxima.

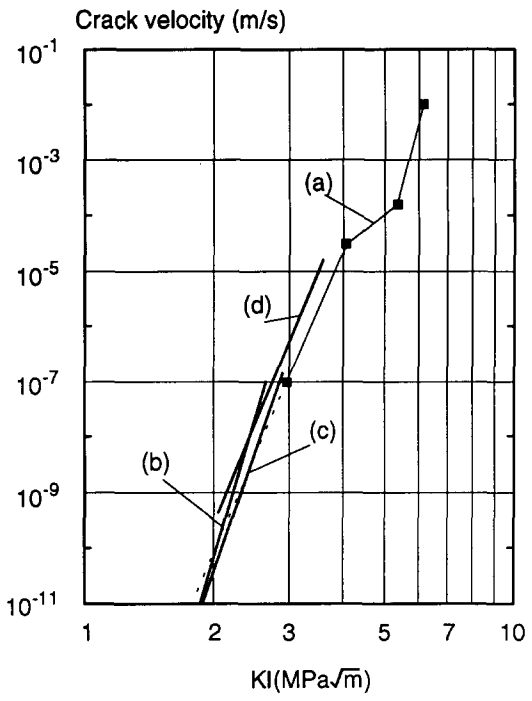

Fig. 7. Subcritical crack growth velocity as a function of the stress intensity factor in the case of the zirconia material. Comparison of results obtained by double torsion (a) (see Ref. 22), by static fatigue using the present analysis (b) and the standard analysis (c) and by dynamic fatigue using the present analysis (d).

3.1.2 Application to mullite

This statistical approach has also been applied to mullite under the same conditions, except the number of specimens, which was lower. The specimens were indented and the initial crack sizes were measured (Table 1). Again it fits a Gaussian law fairly well, but this time with a higher dispersion, since the standard deviation is higher than that obtained with the zirconia material. Thirteen specimens were further loaded to an applied stress of 53 MPa. The results were classified and the same procedure applied to adjust the theoretical curve to the experimental results (Fig. 8). Similarly to zirconia, a range of (A, n) couples can be obtained showing the final uncertainties.

Since the proposed analysis requires the knowledge of the initial crack lengths, it may be argued that a more simple analysis could be conducted by directly applying the relation (8). Indeed, the plot of the time to failure (t_f) as a function of the initial crack length (a_i) on a log–log scale could lead to the determination of the A and n parameters. This analysis has been conducted on the mullite material where the real initial crack lengths have been measured. The results are displayed in Fig. 9. It appears that the correlation coefficient of the regression line is equal to 0·60, which is rather poor, especially compared to that obtained in Fig. 8. This shows that for a given number of specimens the proposed approach gives a better result. This can be

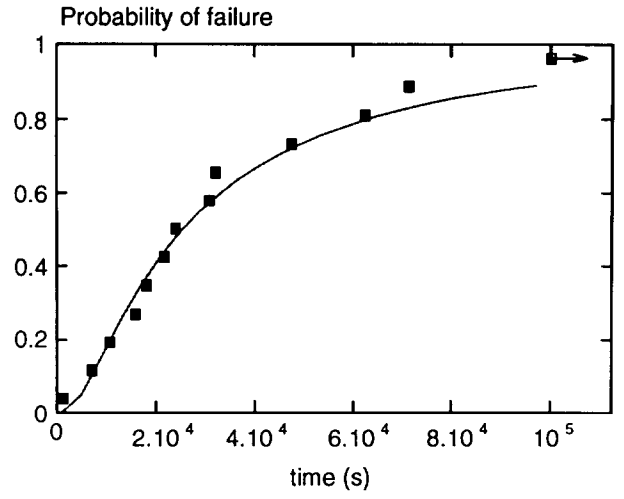

Fig. 8. Fitting of the experimental time to failure by the theoretical probability of failure for the mullite material.

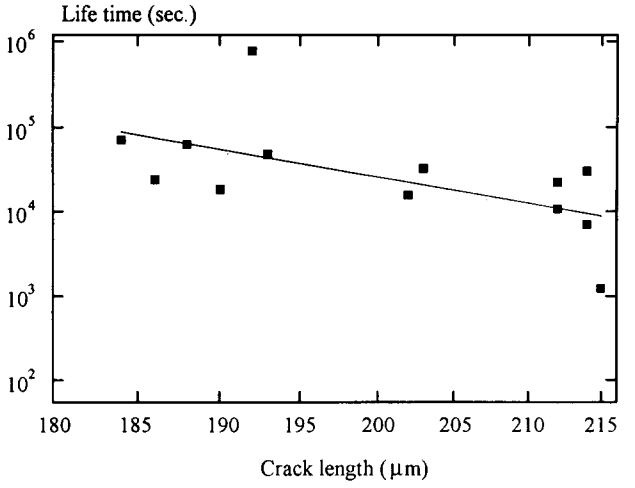

Fig. 9. Representation of the lifetime as a function of the crack size on a log–log plot for the data of the mullite material.

understood by the fact that this method is based on an average distribution of initial flaws, which limits the errors that are otherwise cumulated. Moreover this average distribution can even be improved by measuring a large number of similar artificial flaws made on a single specimen, providing that the different tested samples have the same microstructure.

It should be noted that a relatively precise value of the SCG law can be obtained with a moderate number of specimens. The precision depends on the width of the final distribution, the wider the distribution the higher the precision. This final distribution is, however, not only related to the distribution of initial defects but also to the stress exponent. This is due to the fact that the method is based on the transformation of the initial crack size distribution during the sub-critical crack growth. A large n value or a small value of S_d will decrease the precision.

3.2 Dynamic fatigue

The application of this method to dynamic fatigue has also been conducted.

The difficulty with the standard dynamic fatigue test is the relevance of the data when the real V–K curve shows a typical three stage law. Indeed, the test consists of loading several sets of specimens at different loading rates, for instance in bending. The mathematical analysis of the test[20] shows that under the hypothesis of a single V–K curve, the plot of the logarithm of the apparent strength versus the logarithm of the loading rate defines a straight line related to the A and n parameters (cf. eqn (15)). However, the relative influence of the different stages of the real V–K curve strongly depends on the loading rate.[17] Thus the result of the test will depend on the different loading rates selected and will give some kind of average value. This can be illustrated by conducting a simulation of dynamic fatigue from real data obtained, for instance by double torsion. Figure 10 shows such an example calculated from experimental data obtained on zirconia and mullite. The simulation is, in each case, conducted from results measured by double torsion using the three recorded different stages and also by using the first stage only. Therefore the comparison of both results can show the loading rate range in which the dynamic fatigue test should lead to first stage parameters. Since the parameters corresponding to the first stage are of most importance for prediction and since only these parameters can be solely obtained, it appears that low loading rates should be selected. However, since the standard analysis requires a relatively wide range of loading rates and since extremely low range can not be practically obtained, it cannot lead to correct parameters when a marked three stage law operates.

The statistical analysis proposed in this paper can, however, be used to predict the A_1 and n_1 parameters, since it theoretically requires only one

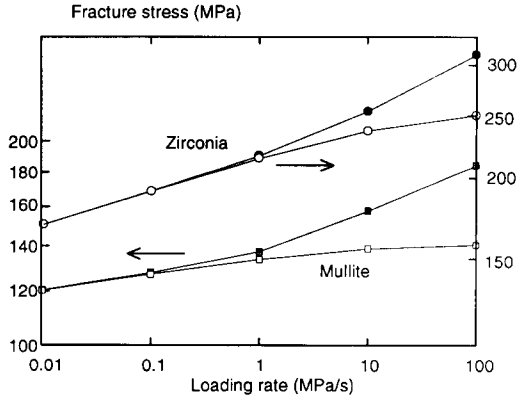

Fig. 10. Results of simulation of dynamic fatigue test from double torsion data of mullite (□, ■) and zirconia (○, ●). ■, ● Simulation conducted with the three stages of the propagation law; □, ○, simulation with the first stage only (Ref. 17).

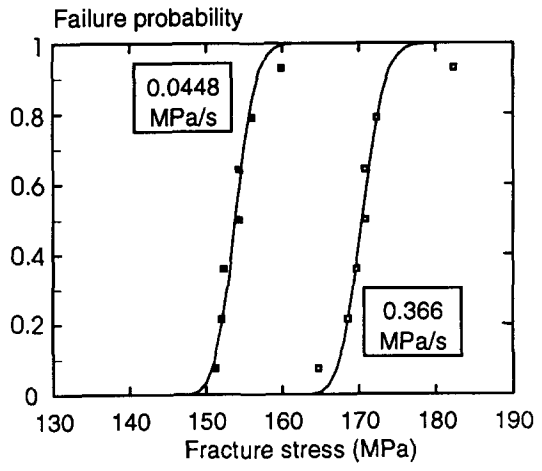

Fig. 11. Fitting of the experimental failure stress by the theoretical probability for the two experimental loading rates. Note that in the case of the lower loading rate, a better accuracy for the determination of A and n is obtained.

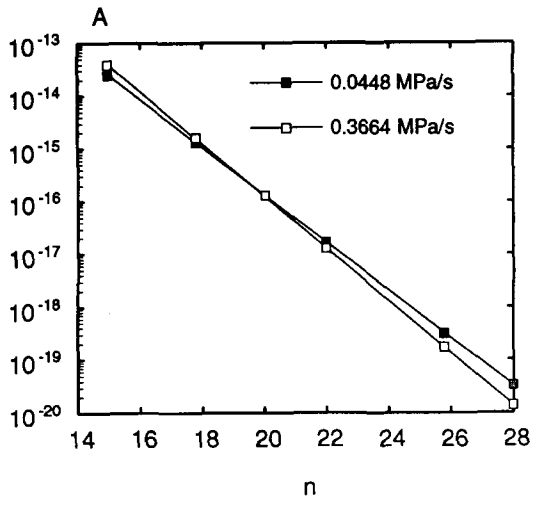

Fig. 12. Representation of the best A parameter value as a function of the n value for both tested loading rates.

loading rate, which can be selected in the proper range.

Such an experiment has been conducted on the zirconia material. It was first aimed to use the first lowest loading rate authorizing the determination of the correct first stage parameters (Fig. 10). For this purpose, seven specimens were indented and tested at a loading rate of 0·366 MPa/s. The same procedure as that described for static fatigue was applied for fitting the experimental results to the theoretical curve. The results in terms of the cumulated probability as a function of the fracture stress are shown in Fig. 11. The same general characteristic of the fitting as for the static test appears, i.e. a wide range of the (A, n) couple can be obtained. However, the range is even larger and it is also important to note that the test duration is too short to significantly modify the initial Gaussian graph, which is still relatively symmetrical.

Therefore a second series of tests was conducted at a lower loading rate of 0·0448 MPa/s. The minimum values of S for a given fixed n value were plotted for both series. In both cases a straight line is again observed but with slightly different slopes (Fig. 12). It might be considered that the intercept of the two lines leads to the most probable (A, n) couples, which in the end leads to the V–K curve represented in Fig. 8. The values are respectively $A = 2{\cdot}25 \times 10^{-17}$ and $n = 19{\cdot}5$. This figure shows that the proposed method can give the parameters of the first stage with only two loading rates with a very good precision.

4 Conclusion

A new statistical method has been developed for the determination of sub-critical crack growth by static fatigue and dynamic fatigue.

This method, which presents the advantage of requiring a single applied stress for the static fatigue test, has been applied to two different materials, zirconia and mullite. It has been shown that relatively precise values could be obtained with a moderate number of specimens. In the case of dynamic fatigue, although the theoretical analysis shows that a single applied loading rate should be necessary, for a high precision, two will generally be required. However, it can still be possible to select relatively low loading rate values in order to obtain results corresponding to the first stage of the propagation law, making the dynamic fatigue test relevant.

It is to be noted that the method requires the knowledge of the initial distribution. A Gaussian law has been applied here in order to fit the indented distribution flaws. A similar procedure could be applied to natural flaws using, for instance, a Weibull distribution.

References

1. Wiederhorn, S. M., Subcritical crack growth in ceramics. In *Fracture Mechanics of Ceramics*, Vol. 2 Plenum Press, New York–London, 1974, pp. 613–46.
2. Pletka, B. J., Fuller, E. R. & Koepke, B. G., An evaluation of double torsion testing—experimental. In *Fracture Mechanics Applied to Brittle Materials*, ASTM STP 678, ed. S. W. Freiman. American Society for Testing and Materials, Philadelphia, PA, 1979, pp. 19–37.
3. Cerkirge, H. H., Tyson, W. R. & Krausz, A. S., Static corrosion and static fatigue of glass. *J. Am. Ceram. Soc.*, **59**(5–6) (1976) 265–6.
4. Champomier, F. P., Crack propagation measurements on glass: a comparison between double torsion and double cantilever beam specimens. In *Fracture Mechanics Applied to Brittle Materials*, ASTM STP 678, ed. S. W. Freiman. American Society for Testing and Materials, Philadelphia, PA, 1979, pp. 60–72.
5. Fett, T. & Munz, D., Evaluation of subcritical crack extension under constant loading. *J. Eur. Ceram. Soc.*, (6) (1990) 67–72.
6. Wiederhorn, S. M., Evans, A. G. & Roberts, D. E., A

fracture mechanics study of the skylab windows. In *Fracture Mechanics of Ceramics*, Vol. 2. Plenum Press, New York–London, 1974, pp. 829–41.
7. Gonzalez, A. C. & Pantano, C. G., A compression-loaded double cantilever bean specimen. *J. Am. Ceram. Soc.*, **73**(8) (1990) 2534–5.
8. Rockar, E. M. & Pletka, B. J., Fracture mechanics of alumina in a simulated biological environment. In *Fracture Mechanics of Ceramics*, Vol. 4. Plenum Press, New York–London, 1978, pp. 725–35.
9. Quinn, S. D., Fracture mechanism maps for advanced structural ceramics. *J. Mat. Sci.*, (25) (1990) 4361–76.
10. Liu, S. Y. & Chen, I. W., Fatigue of yttria-stabilized zirconia. II. Crack propagation, fatigue striations, and short crack behavior. *J. Am. Ceram. Soc.*, **74**(6) (1991) 1206–16.
11. Fett, T., Martin, G., Munz, D. & Thun, G., Determination of da/dN-ΔK_I curves for small cracks in alumina in alternating bending tests. *J. Mat. Sci.*, **26** (1991) 3320–8.
12. Liu, T., Matt, R. & Grathwohl, G., Static and cyclic fatigue of 2Y-TZP ceramics with natural flaws. *J. Eur. Ceram. Soc.*, **11** (1993) 133–41.
13. Jakus, K., Coyne, D. C. & Ritter, J. E., Analysis of fatigue data for lifetime predictions for ceramic materials. *J. Mat. Sci.*, **13** (1978) 2071–80.
14. Fett, T. & Munz, D., Determination of v-K_I curves by a modified evaluation of lifetime measurements in static bending tests. *J. Am. Ceram. Soc.*, **68**(8) (1985) C213–C215.
15. Fett, T., Munz, D. & Keller, K., Determination of subcritical crack growth on glass in water from lifetime measurements on Knoop-cracked specimens. *J. Mat. Sci.*, **23** (1988) 798–803.
16. Fett, T., Germerdonk, K., Grossmuller, A., Munz, D. & Keller, K., Subcritical crack growth and threshold in borosilicate glass. *J. Mat. Sci*, **26** (1991) 253–7.
17. Sudreau, F., Olagnon, C. & Fantozzi, G., Lifetime prediction of ceramics: importance of the test method. *Ceram. Int.*, (1994) **20** (1994) 125–35.
18. Kadouch, O., Rupture différée sous sollicitation mécaniques des ferrites spinelles NiZn et MnZn. PhD Thesis, 1993.
19. Sudreau, F., Olagnon, C., Fantozzi, G. & Leclercq, O., A refined statistical approach for thermal fatigue life prediction. *J. Mat. Sci.*, **27**(5) (1992) 539–46.
20. Ritter, J. E., Engineering design and fatigue failure of brittle materials. In *Fracture Mechanics of Ceramics*, Vol. 4. Plenum Press, New York–London, 1978, pp. 667–87.
21. Fett, T. & Munz, D., Subcritical crack growth of macro- and microcracks in ceramics. In *Fracture Mechanics of Ceramics*, Vol. 9, ed. R. C. Bradt *et al.*. Plenum Press, NY, 1992, pp. 219–33.
22. Chevalier, J., Olagnon, C., Fantozzi, G. & Galès, B., Crack propagation behaviour of Y-TZP ceramics. *J. Am. Ceram. Soc.*, (1993) in press.